# 3D Shape Analysis of the Supraspinatus Muscle

Aaron D. Ward[1], Ghassan Hamarneh[1], Reem Ashry[2], and Mark E. Schweitzer[2]

[1] Medical Image Analysis Lab, Simon Fraser University, Burnaby, BC, V5A 1S6, Canada
{award, hamarneh}@cs.sfu.ca, http://mial.fas.sfu.ca/
[2] Department of Radiology and Orthopedic Surgery, NYU School of Medicine, Hospital for Joint Diseases, New York, NY, 10016, U.S.A.
reem.ashry@gmail.com, mark.schweitzer@nyumc.org

**Abstract.** Pathology of the supraspinatus muscle can involve tearing, which often leads to atrophy and/or retraction of the muscle. Retraction can be corrected through a pull forward operation in surgery, whereas atrophy is generally not correctable. It is therefore important to distinguish between retraction and atrophy. However, since both of these conditions are characterized by a reduction in size, we put forth a pilot study examining changes in 3D shape as they relate to pathological conditions. After segmenting the supraspinatus muscle surface from MRIs representing 57 patients, we compute several different 3D shape measures of the surfaces, and conclude that there are statistically significant differences in shape and size between pathology groups.

## 1 Introduction

The supraspinatus muscle is one of several muscles making up the rotator cuff in the shoulder (figure 1). Disorders of the supraspinatus muscle may involve tearing, which can lead to muscle retraction, atrophy, or both [1]. It is important to be able to distinguish between retraction and atrophy because retraction is a condition that is repairable by pulling the muscle forward in surgery, whereas atrophy is not a condition correctable by surgery. Since both of these conditions result in a reduction of the apparent size of the muscle, 3D shape analysis of the muscle is useful in order to discover shape characterizations that may assist the physician in distinguishing between these groups. Although shoulder arthroscopy is considered the gold standard for the evaluation of the rotator cuff, MR has an exceptionally high accuracy which has been accepted as a standard of reference for several prior papers (e.g. [2–5]).

In this study, we extract the 3D surfaces of the supraspinatus muscle from MRIs of a set of patients. Each patient's data set is labeled according to pathology, forming several groups of patients. For each group, we compute a set of measurements of the 3D surfaces and report the differences observed between the groups.

The remainder of this paper is organized as follows. In sections 2 and 3 we discuss the specifics of the data sets used, and describe our methods for extracting the 3D surface of the muscle and the computation of the shape characteristics

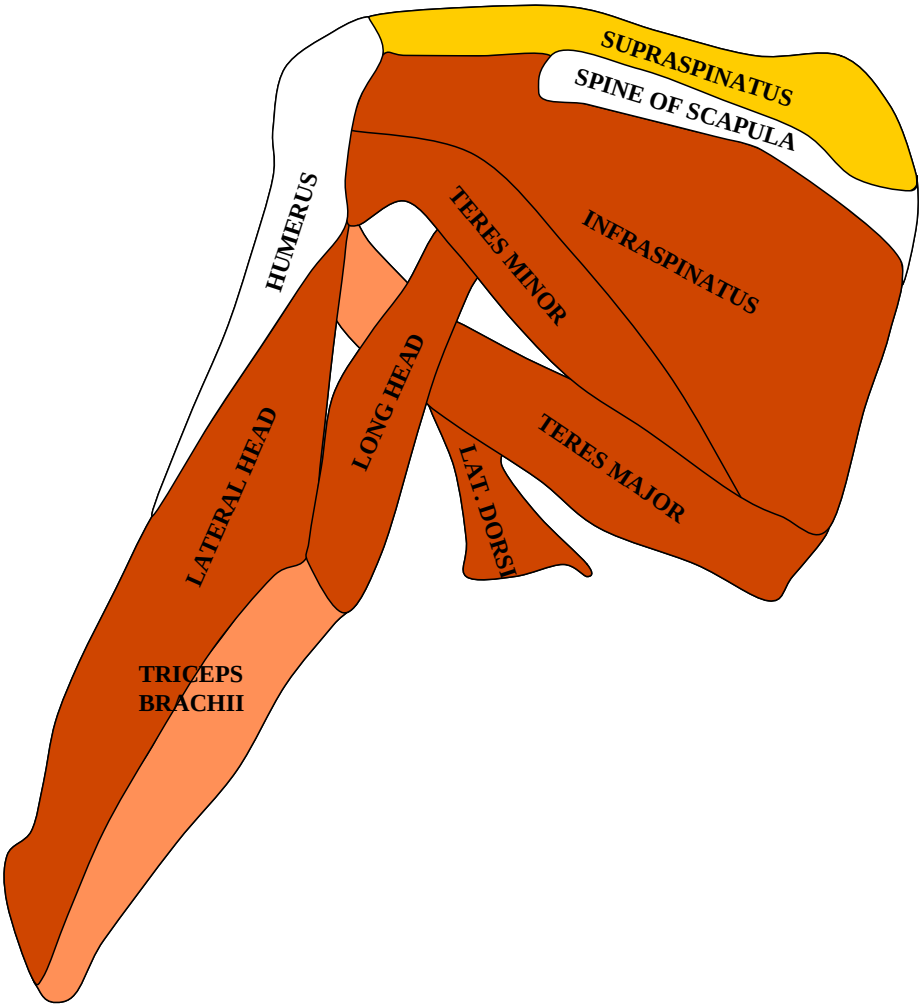


**Fig. 1.** Diagram of shoulder anatomy indicating location of the supraspinatus. Adapted from Grey's Anatomy [6].

of the surfaces. In section 4 we give our results, and in section 5 we make some concluding remarks and give some possible future avenues of research based on this work.

## 2 Material

We acquired MR images of the shoulder from 57 patients at 1.5T. Patients were consistently imaged in supine position, relaxed, and in minimal external rotation in order to normalize for effects of pose and gravity on the shape of the muscle.

The in-plane (sagittal) resolution of the data was 0.3-0.6 mm and the out-of-plane resolution was 3-5 mm. The patients were selected according to diagnoses made by examining the MRIs of the shoulder. The group of patients with torn supraspinati is composed of patients suffering different severities of disease, under the assumption that some of these patients would have visible muscle shape changes and some would not. The retraction group comprises patients with observed relevant mechanical changes to the muscle, and the atrophy group had relevant physiological changes. The control group was composed of patients with unstable shoulders, because they represent a more relevant cross section of the population than would normal subjects.

## 3 Methods

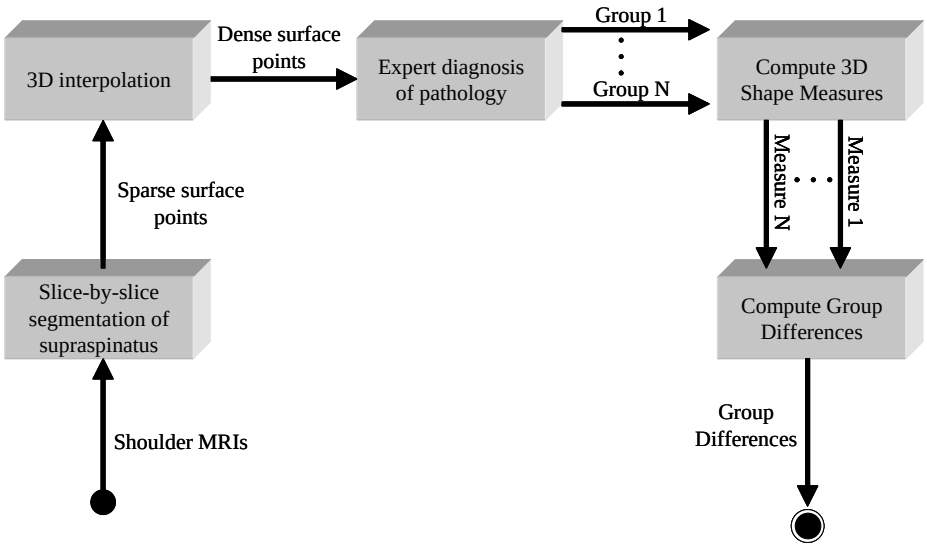


**Fig. 2.** Overall process used in this study. Beginning with a set of 1.5T MRIs of the shoulder, we segment the supraspinatus from each 3D image in a slice-by-slice manner. This yields a set of points that are dense in the imaging plane, but sparse out of the imaging plane due to large intra-slice spacing (figure 3(a)). We then interpolate these points to form a dense set of points forming a 3D surface of the supraspinatus using the Interpolation Module of the segmentation editor in the Amira software (Mercury Computer Systems, Inc) (figure 3(b)). Next, we divide the cases into groups according to expert diagnosis of pathology. We then compute an aggregate (mean) of several 3D shape measures for each group. Finally, we compute and report on differences between the groups.

The overall processing performed on these images is given in figure 2. Expert manual segmentation of the supraspinatus muscle was performed on the sagittal MR images in a slice-by-slice manner. The segmentation tool employed allowed the expert to select control points lying on the surface of the supraspinatus on each slice, and fit a parametric cubic spline curve to these points to guarantee smoothness. The tool performed the spline fitting interactively so that the expert could manipulate the control points until the curve accurately followed the contour of the muscle. It has been shown that intra- and inter-observer variation in supraspinatus contouring is less than 5% [7].

Due to the 3-5 mm inter-slice spacing in the data, the result of this slice-by-slice segmentation is a set of points which are dense within the imaging planes but sparse in the out-of-plane direction (figure 3(a)). 3D interpolation was therefore performed in order to obtain a set of points lying on the object surface that is dense along all axes using the Interpolation Module of the segmentation editor in the Amira software (Mercury Computer Systems, Inc), based on implicit, level-set based shape representation, similar to work by Turk and O'Brien [8] (figure 3(b)).

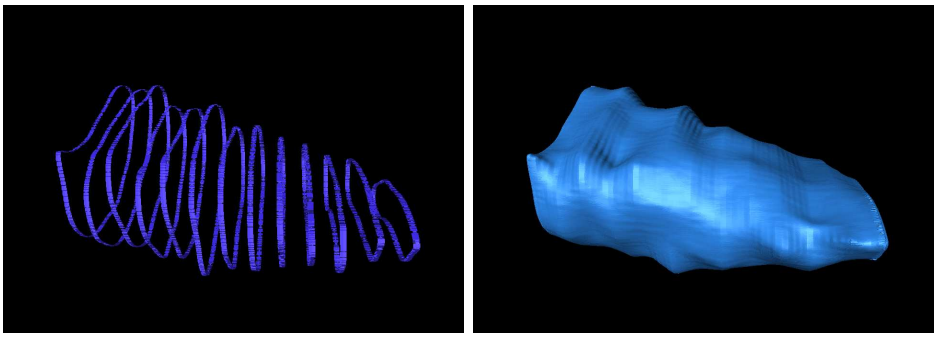

(a) (b)

**Fig. 3.** Supraspinatus muscle surface extraction. (a) Contours resulting from expert segmentation of the supraspinatus, rendered using physical space coordinates. Large spaces between contours are due to the low out-of-plane resolution of the data. (Contours appear non-parallel because of perspective projection.) (b) Result of 3D interpolation of the contours in (a), yielding a dense set of points lying on the surface of the supraspinatus, rendered as a surface.

Next, the condition of the supraspinatus of each patient was assessed by an expert, and assigned to one of the following four groups: normal (N), full thickness tear (T), tear and atrophy (TA), tear and atrophy and retraction (TAR). These four groups represent those for which we wish to compute the shape differences.

We computed 11 different 3D shape measures for each data set:

- **Ratios of eigenvalues (3 measures):** We performed principal components analysis (PCA) [9] against the points lying on the surface of each shape, yielding three eigenvectors and corresponding eigenvalues. The eigenvalues $\lambda_1, \lambda_2, \lambda_3$ represent the variance of the supraspinatus surface points in the direction of the eigenvectors (which describe the main directions of variation) for each supraspinatus. They give an approximation to each supraspinatus by an ellipsoid, where $\lambda_1, \lambda_2, \lambda_3$ represent the lengths of the major axes of such an ellipsoid. Computing the three values of the ratios $\frac{\lambda_1}{\lambda_2}$, $\frac{\lambda_1}{\lambda_3}$, and $\frac{\lambda_2}{\lambda_3}$ yields measures of elongation of the object. For a spherical object we expect that $\lambda_1 \approx \lambda_2 \approx \lambda_3$. For a cylindrical object we expect that $\lambda_1 >> \lambda_2 \approx \lambda_3$, and for a disk-like object we expect that $\lambda_1 \approx \lambda_2 >> \lambda_3$.
- **Mean and standard deviation of distances to centroid (2 measures):** Here, we compute the centroid of all of the supraspinatus surface points, and compute the mean Euclidean distance from each surface point to this centroid, as a measure of size. We also compute the standard deviation of these distances as a measure of surface roughness/non-sphericity.
- **3D moment invariants (3 measures):** We compute three 3D moments that have been shown to be invariant to translation and rotation [10]. They are computed as follows:

$$J_1 = \mu_{200} + \mu_{020} + \mu_{002}$$

$$J_2 = \mu_{200}\mu_{020} + \mu_{200}\mu_{002} + \mu_{020}\mu_{002} - \mu_{110}^2 - \mu_{101}^2 - \mu_{011}^2$$

$$J_3 = \mu_{200}\mu_{020}\mu_{002} + 2\mu_{110}\mu_{101}\mu_{011} - \mu_{002}\mu_{110}^2 - \mu_{020}\mu_{101}^2 - \mu_{200}\mu_{011}^2$$

  where $m_{pqr}$ is the 3D moment and $\mu_{pqr}$ is the 3D central moment as follows:

$$m_{pqr} = \sum_x \sum_y \sum_z x^p y^q z^r p(x,y,z)$$

$$\mu_{pqr} = \sum_x \sum_y \sum_z (x-\bar{x})^p (y-\bar{y})^q (z-\bar{z})^r p(x,y,z)$$

$$\bar{x} = m_{100}/m_{000}$$

$$\bar{y} = m_{010}/m_{000}$$

$$\bar{z} = m_{001}/m_{000}$$

$$p(x,y,z) = \begin{cases} 1 \text{ if } (x,y,z) \text{ is a surface point.} \\ 0 \text{ otherwise.} \end{cases}$$

- **Surface area, volume, and their ratio (3 measures):** We compute the surface area and volume of each supraspinatus in physical units, and take the ratio of surface area to volume.

## 4 Results

Table 1 gives the mean values of the measurements taken for each group. To gain some insight into how these values differ, we computed ratios of measurements of abnormals to normals (table 2). For example, in the first row, we take the mean of the measurements of all abnormal groups to get a single aggregate measure for the abnormals, and take the ratio to the normals. We can see, for example, in the first row of table 2 that the ratio of 0.4 for measurement $J3$ indicates that the mean of the normals was 250% larger than the normals. In subsequent rows of table 2 we give comparisons between specific pathology groups and the normals. For each measurement type, we performed a one-way ANOVA to test the null hypothesis that the means of the normal and pathological groups were the same. The $p$-values resulting from these tests are given in table 4. Measurements with $p$-values rejecting the null hypothesis ($p < 0.05$) are $\frac{\lambda_1}{\lambda 3}$, mean of distances to centroid, the 3D moment invariants, surface area, volume, and the ratio of surface area to volume. From this it appears that characteristics distinguishing normal cases from pathological cases are elongation, size, volume.

## 5 Conclusion

In this work, we presented a pilot study involving 57 cases of varying supraspinatus pathology: normal, tearing, retraction, atrophy, and allowable combinations of these diagnoses. We computed 11 shape characteristics based on 3D points from extracted surface muscles from MRI, and performed a statistical analysis to determine whether or not the measurements of the groups were significantly statistically different. The results indicate that there are significant differences between the groups, and the measures giving the best performance suggest that elongation, surface area and volume are good characterizations of shape for this anatomy.

Future work in this area includes the use of these shape characterizations to train and measure the performance of a classifier attempting to aid in diagnosis of pathology based on the 3D shape of the supraspinatus. Such a classifier would be of great use to a physician attempting to determine whether or not surgery is required to pull the muscle forward (supraspinatus retraction) or if surgery would be ineffective (supraspinatus atrophy). Another interesting area for future study would be to assess the impact on shape analysis of positional difference during imaging (e.g. the influence of internal and external rotation).

## References

1. Robertson, P.L., Schweitzer, M.E., Mitchell, D.G., Schlesinger, F., Epstein, R.E., Frieman, B.G., Fenlin, J.M.: Rotator cuff disorders: interobserver and intraobserver variation in diagnosis with MR imaging. Radiology **194**(3) (1995) 831–835
2. Zlatkin, M., Iannotti, J., Roberts, M., Esterhai, J., Dalinka, M., Kressel, H., Schwartz, J., Lenkinski, R.: Rotator cuff tears: Diagnostic performance of MR imaging. Radiology **172** (1989) 223–229

| | **1** | **2** | **3** | **4** | **5** | **6** | **7** | **8** | **9** | **10** | **11** |
|---|---|---|---|---|---|---|---|---|---|---|---|
| $N$ | 2.4 | 5.7 | 2.5 | 2.0 | 0.7 | $1.2 \times 10^5$ | $5.3 \times 10^9$ | $7.6 \times 10^{13}$ | 77.0 | 24.8 | 0.3 |
| $T$ | 2.6 | 6.7 | 2.6 | 1.8 | 0.6 | $8.7 \times 10^4$ | $2.7 \times 10^9$ | $2.6 \times 10^{13}$ | 62.1 | 16.3 | 0.2 |
| $TA$ | 4.0 | 10.4 | 2.7 | 1.8 | 0.7 | $6.5 \times 10^4$ | $1.5 \times 10^9$ | $1.3 \times 10^{13}$ | 58.2 | 13.7 | 0.2 |
| $TAR$ | 3.0 | 7.4 | 3.0 | 1.6 | 0.6 | $3.7 \times 10^4$ | $4.6 \times 10^8$ | $1.7 \times 10^{12}$ | 42.7 | 7.9 | 0.2 |

**Table 1.** Mean values of each of the measurements for each of the groups. Refer to table 3 for meanings of the numbered column headings.

| | **1** | **2** | **3** | **4** | **5** | **6** | **7** | **8** | **9** | **10** | **11** |
|---|---|---|---|---|---|---|---|---|---|---|---|
| *mean(Abnormal)/N* | 1.2 | 1.3 | 1.1 | 0.9 | 0.9 | 0.7 | 0.5 | 0.4 | 0.8 | 0.6 | 0.8 |
| *T/N* | 1.1 | 1.2 | 1.1 | 0.9 | 0.9 | 0.7 | 0.5 | 0.3 | 0.8 | 0.7 | 0.8 |
| *TA/N* | 1.6 | 1.8 | 1.1 | 0.9 | 1.0 | 0.6 | 0.3 | 0.2 | 0.8 | 0.6 | 0.7 |
| *TAR/N* | 1.2 | 1.3 | 1.2 | 0.8 | 0.8 | 0.3 | 0.09 | 0.02 | 0.6 | 0.3 | 0.6 |

**Table 2.** Comparison of the mean values of the measurements for each group. The values in the first row are computed by first taking the mean of the measurements across all abnormal groups. We then take the ratio of the mean measurement for the abnormals to the mean of the normals. The remaining rows show the ratios for all of the individual abnormal groups. Refer to table 3 for meanings of the numbered column headings.

| *Measurement number* | *Description* |
|---|---|
| 1 | $\lambda_1$ / $\lambda_2$ |
| 2 | $\lambda_1$ / $\lambda_3$ |
| 3 | $\lambda_2$ / $\lambda_3$ |
| 4 | Mean of distances to centroid (cm) |
| 5 | Standard deviation of distances to centroid (cm) |
| 6 | $J_1$ |
| 7 | $J_2$ |
| 8 | $J_3$ |
| 9 | Surface area ($cm^2$) |
| 10 | Volume ($cm^3$) |
| 11 | Surface area / Volume (1 / cm) |

**Table 3.** Meanings of the column headings given in tables 1 and 2. This legend is given in a separate table here due to space considerations.

| | **1** | **2** | **3** | **4** | **5** | **6** | **7** | **8** | **9** | **10** | **11** |
|---|---|---|---|---|---|---|---|---|---|---|---|
| *p-value* | 0.0733 | 0.0071 | 0.5849 | 0.0198 | 0.3304 | 0.0093 | 0.0118 | 0.0129 | 0.0010 | 0.0007 | 0.00001 |

**Table 4.** p-values resulting from one-way ANOVA test for each measurement, testing the null hypothesis that the means of all of the groups are the same. Refer to table 3 for meanings of the numbered column headings.

3. Bachmann, G.F., Melzer, C., Heinrichs, C.M., Moehring, B., Rominger, M.B.: Diagnosis of rotator cuff lesions: Comparison of US and MRI on 38 joint specimens. European Radiology **7**(2) (1997) 192–197
4. Quinn, S.F., Sheley, R.C., Demlow, T.A., Szumowski, J.: Rotator cuff tendon tears: Evaluation with fat-suppressed MR imaging with arthroscopic correlation in 100 patients. Radiology **195** (1995) 497–500
5. Swen, W.A.A., Jacobs, J.W.G., Algra, P.R., Manoliu, R.A., Rijkmans, J., Willems, W.J., Bijlsma, J.W.J.: Sonography and magnetic resonance imaging equivalent for the assessment of full-thickness rotator cuff tears. Arthritis and Rheumatism **42**(10) (1999) 2231–2238
6. Gray, H.: Anatomy of the Human Body, 20th ed. Lea and Febiger, Philadelphia, U.S.A. (1918)
7. Lehtinen, J.T., Tingart, M.J., Apreleva, M., Zurakowski, D., Palmer, W., Warner, J.J.: Practical assessment of rotator cuff muscle volumes using shoulder MRI. Acta Orthop Scand **74**(6) (2003) 722–729
8. Turk, G., O'Brien, J.F.: Shape transformation using variational implicit functions. Proceedings of ACM SIGGRAPH (1999) 335–342
9. Jolliffe, I.T.: Principal Components Analysis. Springer-Verlag, New York, U.S.A. (1986)
10. Sadjadi, F.A., Hall, E.L.: Three-dimensional moment invariants. IEEE PAMI **2**(2) (1980) 127–136